

# The new streamline diffusion for the 3D coupled Schrödinger equations with a cross-phase modulation

Davood Rostamy<sup>1</sup>

(Received 20 April 2013; revised 5 December 2013)

## Abstract

We study the new streamline diffusion finite element method for treating the three dimensional coupled nonlinear Schrödinger equation. We derive stability estimates and optimal convergence rates. Moreover, an a priori error estimate is obtained and we compare the corresponding optimal convergence rate for popular numerical methods such as conservative finite difference, semi-implicit finite difference, semi-discrete finite element and the time-splitting spectral method. We justify the advantage of the streamline diffusion method versus the some numerical methods with some examples. Test problems are presented to verify the efficiency and accuracy of the method. The results reveal that the proposed scheme is very effective, convenient and quite accurate for such considered problems rather than other methods.

---

<http://journal.austms.org.au/ojs/index.php/ANZIAMJ/article/view/6990> gives this article, © Austral. Mathematical Soc. 2013. Published December 30, 2013. ISSN 1446-8735. (Print two pages per sheet of paper.) Copies of this article must not be made otherwise available on the internet; instead link directly to this URL for this article.

*Keywords:* Streamline diffusion methods, coupled nonlinear Schrödinger equations, finite element, stability, convergence analysis.

# Contents

|          |  |            |
|----------|--|------------|
| <b>1</b> | <b>Introduction</b>                                  | <b>E52</b> |
| <b>2</b> | <b>Streamline diffusion method</b>                   | <b>E56</b> |
| 2.1      | Bézier elements . . . . .                            | E56        |
| 2.2      | The new streamline diffusion . . . . .               | E57        |
| <b>3</b> | <b>Stability for the streamline diffusion method</b> | <b>E59</b> |
| <b>4</b> | <b>Experimental results</b>                          | <b>E63</b> |
| <b>5</b> | <b>Conclusion</b>                                    | <b>E74</b> |
|          | <b>References</b>                                    | <b>E74</b> |

## 1 Introduction

Developing new numerical ideas for approximation of the solutions of nonlinear Schrödinger equations is an interesting research area of many engineers and mathematicians. Also, the coupled nonlinear Schrödinger equations (CNLSE) is obtained in a great variety of physical situations [33, 34]. For example, in fiber system, such equations have been shown to govern pulse propagation along orthogonal polarization axes [10, 11, 19, 24, 33, 34]. Also, these equations model beam propagation inside photo or crystals refractives as well as water wave effects [33, 34]. Solitary waves are called vector solitons as they generally contain two parts. In all the above physical situations, collision of vector solitons is an important issue. In addition to passing-through collision is an

important phenomena such that vector solitons also bounce off each other or trap each other. Solutions of this system have been studied intensively in recent years in numerical aspects and analytical [19, 20, 21, 22, 23, 24, 31, 32, 33, 34, 35, 36, 37]. Numerical examples were investigated by many authors in the one dimensional case [21, 21, 22, 23, 24, 34]. But in three dimensional case, many numerical methods are unstable [7, 8, 9, 10]. Therefore, we need to give a stable method for solving this class of equation in three dimensions.

Streamline diffusion methods have been considered by many [2, 3, 4, 5, 6, 12, 13, 14, 15, 16, 17, 18, 25, 26, 27, 28, 29, 30]. These methods are alternative numerical approaches to the classical numerical methods such as the finite element and boundary element method. They have attracted much attention in recent years because of their flexibility and simplicity. These methods perform slightly better than the standard finite element methods for smooth solutions and non-smooth solutions to hyperbolic problems in three dimensions [7, 8, 9, 10]. Contrived diffusion is joined only in the characteristic direction so that internal layers are not smeared out, while the added diffusion takes off oscillations near boundary layers.

We consider the example of the three dimensional coupled nonlinear Schrödinger equations (CNLSE) [34]:

$$\begin{aligned} i \frac{\partial \psi_1}{\partial t} + \frac{1}{2} \Delta_x \psi_1 + (|\psi_1|^2 + e(t)|\psi_2|^2) \psi_1 &= 0, \\ i \frac{\partial \psi_2}{\partial t} + \frac{1}{2} \Delta_x \psi_2 + (e(t)|\psi_1|^2 + |\psi_2|^2) \psi_2 &= 0, \end{aligned} \quad (1)$$

where  $\Delta_x = \sum_{j=1}^3 \frac{\partial^2}{\partial x_j^2}$ ,  $\nabla_x = (\frac{\partial}{\partial x_1}, \frac{\partial}{\partial x_2}, \frac{\partial}{\partial x_3})$  and  $\mathbf{x} = (x_1, x_2, x_3) \in \mathbb{R}^3$ . Also,  $\psi_1$  and  $\psi_2$  are the wave amplitudes in two polarizations and  $e(t)$  is the cross-phase modulation coefficient. The initial condition is

$$\psi_1(\mathbf{x}, 0) = g_1(\mathbf{x}), \quad \psi_2(\mathbf{x}, 0) = g_2(\mathbf{x}), \quad (2)$$

and boundary condition is

$$|\nabla_x \psi_1(\mathbf{x}, t)| = |\nabla_x \psi_2(\mathbf{x}, t)| = 0 \text{ as } |\mathbf{x}| \rightarrow \infty. \quad (3)$$

We assume that the solution of the system (1) is negligibly small outside the cube  $\mathcal{C} = [x_L, x_R] \times [x_L, x_R] \times [x_L, x_R]$ , and so we consider the coupled nonlinear Schrödinger equations

$$\begin{aligned} i \frac{\partial \psi_1}{\partial t} + \frac{1}{2} \Delta_x \psi_1 + (|\psi_1|^2 + e(t)|\psi_2|^2) \psi_1 &= 0, \\ i \frac{\partial \psi_2}{\partial t} + \frac{1}{2} \Delta_x \psi_2 + (e(t)|\psi_1|^2 + |\psi_2|^2) \psi_2 &= 0, \end{aligned}$$

in the domain  $\mathcal{C}$ , with initial conditions

$$\psi_1(x, 0) = g_1(x), \quad \psi_2(x, 0) = g_2(x),$$

and boundary conditions

$$|\nabla_x \psi_1(x, t)| = |\nabla_x \psi_2(x, t)| = 0, \quad x \in \partial \mathcal{C}.$$

We decompose the complex functions  $\psi_1$  and  $\psi_2$  in the CNLSE into its real and imaginary parts by writing

$$\psi_1(x, t) = u_1 + iu_2, \quad \psi_2(x, t) = u_3 + iu_4,$$

where  $u_j$ ,  $j = 1, \dots, 4$ , are real functions. Therefore, we explore the system

$$\begin{aligned} \frac{\partial u_1}{\partial t} + \frac{1}{2} \Delta_x u_2 + z_1 u_2 &= 0, \\ \frac{\partial u_2}{\partial t} - \frac{1}{2} \Delta_x u_1 - z_1 u_1 &= 0, \\ \frac{\partial u_3}{\partial t} + \frac{1}{2} \Delta_x u_4 + z_2 u_4 &= 0, \\ \frac{\partial u_4}{\partial t} - \frac{1}{2} \Delta_x u_3 - z_2 u_3 &= 0, \end{aligned}$$

where we define

$$\begin{aligned} z_1 &= u_1^2 + u_2^2 + e(t)(u_3^2 + u_4^2), \\ z_2 &= e(t)(u_1^2 + u_2^2) + u_3^2 + u_4^2. \end{aligned}$$

The above system in a matrix-vector form is

$$\begin{aligned} \mathbf{u}_t - \frac{1}{2} \mathbf{A} \Delta \mathbf{u} + \mathbf{F}(\mathbf{u}) \mathbf{u} &= \mathbf{0} \quad \text{in } (\mathcal{C} \times [\mathbf{0}, \mathbf{T}]), \\ \mathbf{u}(\mathbf{x}, 0) &= \mathbf{u}_0 \quad \text{on } \mathbf{x} \in \mathcal{C}, \\ \nabla \mathbf{u} &= \mathbf{0}, \quad \mathbf{x} \in \partial \mathcal{C}, \end{aligned} \quad (4)$$

where  $\mathbf{u}_t = \frac{\partial \mathbf{u}}{\partial t}$ ,  $\Delta \mathbf{u} = \Delta_x \mathbf{u}$ ,  $\nabla \mathbf{u} = (\nabla_x \mathbf{u}_1, \nabla_x \mathbf{u}_2, \nabla_x \mathbf{u}_3, \nabla_x \mathbf{u}_4)^\top$ ,

$$\mathbf{u} = \begin{bmatrix} \mathbf{u}_1 \\ \mathbf{u}_2 \\ \mathbf{u}_3 \\ \mathbf{u}_4 \end{bmatrix}, \quad \mathbf{A} = \begin{bmatrix} 0 & -1 & 0 & 0 \\ 1 & 0 & 0 & 0 \\ 0 & 0 & 0 & -1 \\ 0 & 0 & 1 & 0 \end{bmatrix}, \quad \mathbf{F}(\mathbf{u}) = \begin{bmatrix} 0 & z_1 & 0 & 0 \\ -z_1 & 0 & 0 & 0 \\ 0 & 0 & 0 & z_2 \\ 0 & 0 & -z_2 & 0 \end{bmatrix},$$

and if in (2), we have  $\mathbf{g}_j(\mathbf{x}) = \mathbf{g}_{j1}(\mathbf{x}) + i\mathbf{g}_{j2}(\mathbf{x})$  for  $j = 1, 2$ , then  $\mathbf{u}_0 = [\mathbf{g}_{11}, \mathbf{g}_{12}, \mathbf{g}_{21}, \mathbf{g}_{22}]^\top$ . Yang [33] studied analytically the linear stability of two-vector solitons bound states in the coupled NLS equations by a tail-matching method. He obtained some conditions for small eigenvalues and he showed that these bound states are always linearly unstable due to the existence of one unstable phase-induced eigenvalue.

Also, the stability properties of such solutions for external perturbations as well as during interactions among themselves have been studied both numerically [20, 23] and analytically [33]. For example, numerical simulations of the propagation and interactions of one-dimensional Langmuir solitons and their generation from random fluctuations by an external pump field were presented by Ismail and Taha [20, 21, 22, 23, 24].

Recently, various numerical methods such as finite difference methods [22], the finite element (FE) method [23], continuous Galerkin (CG) method [20], discontinuous Galerkin (DG) method [31], and discontinuous Petrov–Galerkin (DPG) with optimal test functions [37] have been widely used to solve this problem. However, to the best of our knowledge, only some did numerical work concerning these coupled equations using the finite difference Crank–Nicolson (CN) scheme and the standard finite element method, while the

intensive analysis of the precision of this method is very limited. Hence, it is of great interests to develop an efficient and accurate method for these equations. Therefore, Section 2 defines slabs for the space-time domain and obtains the SD-method for (4) and Section 3 studies stability estimates and proves convergence rates for the streamline diffusion approximation of the CNLSE. Computational results are given in Section 4, and finally conclusions are given in Section 5.

## 2 Streamline diffusion method

### 2.1 Bézier elements

The  $p + 1$  Bernstein basis polynomial of degree  $k$  are defined for  $t \in [0, T]$  as

$$\mathcal{B}_{i,k}(t) = \binom{k}{i} t^i \frac{(T-t)^{k-i}}{T^k}, \quad i = 0, \dots, k. \quad (5)$$

These constitute a basis of the polynomials of degree  $k$  and are pointwise non-negative. The motivation for performing finite element computation using this basis is that a piecewise Bernstein polynomial basis is mapped onto a B-spline basis by invoking the Bézier extraction operator [36]. This transformation enables the representation of a NURBS (i.e., non uniform rational basis spline) or a T-spline by using a set of Bézier elements. Therefore, we consider a Bézier curve of degree  $p$  that is defined by a linear combination of  $k + 1$  Bernstein polynomial basis functions. We define the set of basis functions as  $\mathcal{B}(t) = \{\mathcal{B}_{i,k}(t)\}_{i=1}^{k+1}$ , and the corresponding set of vector-valued control points as  $\mathbf{P} = \{\mathbf{P}_i\}_{i=1}^{p+1}$  where each  $\mathbf{P}_i \in \mathbb{R}^d$ ,  $d$  being the number of spatial dimensions, and  $\mathbf{P}$  is a matrix of dimension  $(k + 1) \times d$ ; that is,  $\mathbf{P} = \{\mathbf{P}_i^j\}_{i,j=1}^{k+1,d}$ . Hence, the Bézier curve is

$$\mathbf{R}_k(t) = \sum_{i=1}^{k+1} \mathbf{P}_i \mathcal{B}_{i,k}(t), \quad t \in [0, T].$$

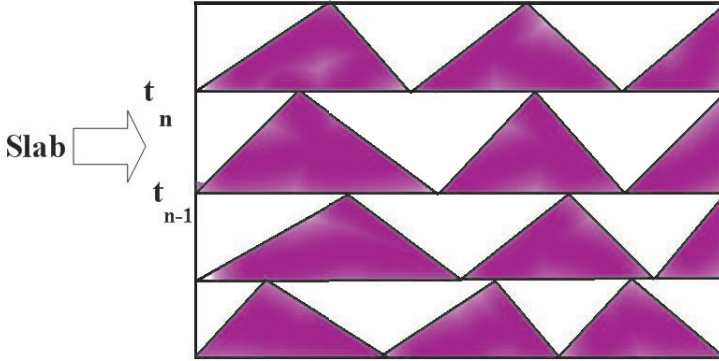


Figure 1: The slabs on Rectangle when the horizontal line shows  $X = \frac{1}{3} \sum_{j=1}^3 x_j$

## 2.2 The new streamline diffusion

This section considers the SD-method for solving (4) that is based on using finite element over the space-time domain  $\Omega = \mathcal{C} \times [0, T]$ . To define this method, let  $0 = t_0 < t_1 < \dots < t_N = T$  be a subdivision of the time interval  $[0, T]$  into intervals  $I_n = (t_n, t_{n+1})$ , with time steps  $k_n = t_{n+1} - t_n$ ,  $n = 0, 1, \dots, N - 1$ , and introduce the corresponding space-time slabs (see Figure 1), that is,

$$S_n = \{(x, t) : x \in \mathcal{C}, t_n \leq t < t_{n+1}\}, \tag{6}$$

for  $n = 0, 1, \dots, N - 1$ . Further, for each  $n$  let  $U^n$  be a finite element subspace of  $(L_2(S_n))^4$ . Summing over  $n$ , taking all the slabs together we get the function space  $U = \prod_{n=0}^{N-1} U^n$ . For  $h > 0$ , we define  $T_h^n$  such that be a triangulation of the slab  $S_n$  into triangles  $K$  satisfying as usual the minimum angle condition [9] and assume that the parameter  $h$  is represented with the maximum diameter of the triangles  $K \in T_h^n$ . We introduce

$$U_h^n = \{u \in U^n : u|_K \in (R_k(K))^4 \text{ for } K \in T_h^n\},$$

where  $R_k(K)$  denotes the set of Bézier polynomials in  $K$  of degree less than or equal  $k$  and we define the function space that summing over  $n$ , taking all the

slabs together,

$$\mathbf{u}_h = \prod_{n=0}^{N-1} \mathbf{u}_h^n.$$

We use the following notation. Given a domain  $\Omega$ , we denote  $(\cdot, \cdot)_\Omega$  as the usual  $L_2(\Omega)$  scalar product,  $\|\cdot\| = \|\cdot\|_{L_2(\Omega)}$  the corresponding  $L_2$  norm, and for a positive integer  $k$ ,  $H^k(\Omega)$  denote the usual Sobolev space of functions with square integrable derivative of order less than or equal  $k$  with norm  $\|\cdot\|_{k,\Omega}$  [1]. We formulate the SD-method on the slab  $S_n$  for (4), as follows.

For  $n = 0, \dots, N - 1$ , find  $\mathbf{u}_h^n \in \mathbf{U}_h^n$  such that

$$\begin{aligned} & [\mathbf{u}_{h,t}^n + \mathbf{F}(\mathbf{u}_h^n)\mathbf{u}_h^n, \mathbf{g} + \delta(\mathbf{g}_t + \mathbf{F}(\mathbf{u}_h^n)\mathbf{g})]_n + \frac{1}{2}(\mathbf{A}\nabla\mathbf{u}_h^n, \nabla\mathbf{g})_n \\ & - \frac{1}{2}\delta[\mathbf{A}\Delta\mathbf{u}_h^n, \mathbf{g}_t + \mathbf{F}(\mathbf{u}_h^n)\mathbf{g}]_n + \langle \mathbf{u}_{h,+}^n, \mathbf{g}_+ \rangle_n = \langle \mathbf{u}_{h,-}^n, \mathbf{g}_+ \rangle_n. \end{aligned} \quad (7)$$

Where  $\delta = \bar{C}h$  with  $\bar{C}$  is a suitable chosen (sufficiently small, [28]) positive constant. Further, we define the following notations for (7):

$$\begin{aligned} (\mathbf{u}, \mathbf{g})_n &= \int_{S_n} \mathbf{u}^T \cdot \mathbf{g} \, dx \, dt, \\ (\mathbf{u}, \mathbf{g})_\Omega &= \sum_{n=0}^{N-1} (\mathbf{u}, \mathbf{g})_n, \\ \langle \mathbf{u}, \mathbf{g} \rangle_n &= \int_{\Omega} \mathbf{u}^T(x, t_n) \cdot \mathbf{g}(x, t_n) \, dx, \\ \mathbf{u}_+(x, t) &= \lim_{s \rightarrow 0^+} \mathbf{u}(x, t + s), \\ \mathbf{u}_-(x, t) &= \lim_{s \rightarrow 0^-} \mathbf{u}(x, t + s). \end{aligned}$$



We introduce the following notation:

$$\begin{aligned}
 B(F(\tilde{\mathbf{u}}); \mathbf{u}, \mathbf{g}) &= \sum_{n=0}^{N-1} \left[ (\mathbf{u}_t + F(\tilde{\mathbf{u}})\mathbf{u}, \mathbf{g} + \delta(\mathbf{g}_t + F(\mathbf{u}_h)\mathbf{g}))_n + \frac{1}{2}(A\nabla\mathbf{u}, \nabla\mathbf{g})_n \right. \\
 &\quad \left. - \frac{1}{2}\delta(A\Delta\mathbf{u}, \mathbf{g}_t + F(\mathbf{u}_h)\mathbf{g})_n \right] + \sum_{n=1}^{N-1} \langle [\mathbf{u}], \mathbf{g}_+ \rangle_n + \langle \mathbf{u}_+, \mathbf{g}_+ \rangle_0, \tag{8}
 \end{aligned}$$

and the linear form

$$L(\mathbf{g}) = \langle \mathbf{u}_0, \mathbf{g}_+ \rangle_0.$$

Where we define  $\mathbf{u} = (\mathbf{u}_1, \mathbf{u}_2, \mathbf{u}_3, \mathbf{u}_4)^T$  and  $[\mathbf{u}] = ([\mathbf{u}_1], [\mathbf{u}_2], [\mathbf{u}_3], [\mathbf{u}_4])^T$  such that for  $\mathbf{q} = \mathbf{u}_i$ ,  $i = 1, 2, 3, 4$ , we have  $[\mathbf{q}] = \mathbf{q}_+ - \mathbf{q}_-$ . Observe that  $\mathbf{u}_h$  depends on  $B$  in the first term on the right hand side of (8). Now the problem (7) is more concisely formulated as follows.

Find  $\mathbf{u}_h \in \mathbf{U}_h$  such that, for  $\mathbf{g} \in \mathbf{U}_h$ ,

$$B(F(\mathbf{u}_h); \mathbf{u}_h, \mathbf{g}) = L(\mathbf{g}). \tag{9}$$

### 3 Stability for the streamline diffusion method

This section concludes the stability estimate for the SD-method (9). These estimate are of crucial importance in proving the finite element analysis. From the generalized Lax–Milgram lemma, we know that the problem has a unique solution, if the conditions are satisfied in Proposition 1 also, then we investigate some properties of  $B$ .

**Proposition 1.** For any  $\mathbf{g} \in \mathbf{U}$ ,

$$B(F(\mathbf{u}_h); \mathbf{g}, \mathbf{g}) \geq \frac{1}{2} \|\mathbf{g}\|^2, \tag{10}$$

with the norm  $\|\cdot\|$  defined as

$$\|\mathbf{g}\|^2 = \frac{1}{2} \left\{ |\mathbf{g}_-|_{\Omega}^2 + |\mathbf{g}_+|_0^2 + \sum_{n=1}^{N-1} |[\mathbf{g}]_n|^2 + 2\delta \|\mathbf{g}_t + \mathbf{F}(\mathbf{u}_h)\mathbf{g}\|_{\Omega}^2 + 2\|\nabla\mathbf{g}\|_{\Omega}^2 \right\}. \quad (11)$$

**Proof:** Using the definition of the form  $B$  and setting  $\mathbf{u} = \mathbf{g}$

$$\begin{aligned} B(\mathbf{F}(\mathbf{u}_h); \mathbf{g}, \mathbf{g}) &= (\mathbf{g}_t, \mathbf{g})_{\Omega} + (\mathbf{F}(\mathbf{u}_h)\mathbf{g}, \mathbf{g})_{\Omega} + \delta \|\mathbf{g}_t + \mathbf{F}(\mathbf{u}_h)\mathbf{g}\|_{\Omega}^2 \\ &\quad + \frac{1}{2} (\mathbf{A}\nabla\mathbf{g}, \nabla\mathbf{g})_{\Omega} - \frac{1}{2} \delta (\mathbf{A}\Delta\mathbf{g}, \mathbf{g}_t + \mathbf{F}(\mathbf{u}_h)\mathbf{g})_{\Omega} \\ &\quad + \sum_{n=1}^{N-1} \langle [\mathbf{g}], \mathbf{g}_+ \rangle_n + \langle \mathbf{g}_+, \mathbf{g}_+ \rangle_0. \end{aligned} \quad (12)$$

Integrating by parts yields

$$(\mathbf{g}_t, \mathbf{g})_{\Omega} + \sum_{n=1}^{N-1} \langle [\mathbf{g}], \mathbf{g}_+ \rangle_n + \langle \mathbf{g}_+, \mathbf{g}_+ \rangle_0 = \frac{1}{2} \left\{ |\mathbf{g}_-|_{\Omega}^2 + |\mathbf{g}_+|_0^2 + \sum_{n=1}^{N-1} |[\mathbf{g}]_n|^2 \right\}. \quad (13)$$

By using the definitions,


$$\begin{aligned} (\mathbf{F}(\mathbf{u}_h)\mathbf{g}, \mathbf{g})_{\Omega} &= \int_{\Omega} \left( \begin{bmatrix} 0 & z_{1,h} & 0 & 0 \\ -z_{1,h} & 0 & 0 & 0 \\ 0 & 0 & 0 & z_{2,h} \\ 0 & 0 & -z_{2,h} & 0 \end{bmatrix} \begin{bmatrix} g_1 \\ g_2 \\ g_3 \\ g_4 \end{bmatrix} \right) \cdot \begin{bmatrix} g_1 \\ g_2 \\ g_3 \\ g_4 \end{bmatrix} ds \\ &= \int_{\Omega} \begin{bmatrix} z_{1,h}g_2 & -z_{1,h}g_1 & z_{2,h}g_4 & -z_{2,h}g_3 \end{bmatrix} \cdot \begin{bmatrix} g_1 \\ g_2 \\ g_3 \\ g_4 \end{bmatrix} ds \\ &= \int_{\Omega} (z_{1,h}g_2g_1 - z_{1,h}g_1g_2 + z_{2,h}g_4g_3 - z_{2,h}g_3g_4) ds = 0, \end{aligned} \quad (14)$$

and

$$\begin{aligned}
 (A\nabla\mathbf{g}, \nabla\mathbf{g})_{\Omega} &= \int_{\Omega} \left( \begin{bmatrix} 0 & -1 & 0 & 0 \\ 1 & 0 & 0 & 0 \\ 0 & 0 & 0 & -1 \\ 0 & 0 & 1 & 0 \end{bmatrix} \begin{bmatrix} \frac{\partial g_1}{\partial x} \\ \frac{\partial g_2}{\partial x} \\ \frac{\partial g_3}{\partial x} \\ \frac{\partial g_4}{\partial x} \end{bmatrix} \right) \cdot \begin{bmatrix} \frac{\partial g_1}{\partial x} \\ \frac{\partial g_2}{\partial x} \\ \frac{\partial g_3}{\partial x} \\ \frac{\partial g_4}{\partial x} \end{bmatrix} ds \\
 &= \int_{\Omega} \begin{bmatrix} -\frac{\partial g_2}{\partial x} & \frac{\partial g_1}{\partial x} & -\frac{\partial g_4}{\partial x} & \frac{\partial g_3}{\partial x} \end{bmatrix} \cdot \begin{bmatrix} \frac{\partial g_1}{\partial x} \\ \frac{\partial g_2}{\partial x} \\ \frac{\partial g_3}{\partial x} \\ \frac{\partial g_4}{\partial x} \end{bmatrix} ds \\
 &= \int_{\Omega} \left( -\frac{\partial g_2}{\partial x} \frac{\partial g_1}{\partial x} + \frac{\partial g_2}{\partial x} \frac{\partial g_1}{\partial x} - \frac{\partial g_3}{\partial x} \frac{\partial g_4}{\partial x} + \frac{\partial g_3}{\partial x} \frac{\partial g_4}{\partial x} \right) ds = 0.
 \end{aligned} \tag{15}$$

By the inverse inequality and the inequality  $2ab \leq \epsilon a^2 + \epsilon^{-1}b^2$  for  $a, b$  real numbers and  $\epsilon > 0$ ,

$$\begin{aligned}
 \frac{1}{2}\delta |(A\Delta\mathbf{g}, \mathbf{g}_t + F(\mathbf{u}_h)\mathbf{g})_{\Omega}| &\leq \frac{1}{4} (\|\nabla\mathbf{g}\|_{\Omega}^2 + \delta\|\mathbf{g}_t + F(\mathbf{u}_h)\mathbf{g}\|_{\Omega}^2) \\
 &\leq \frac{1}{4}\|\mathbf{g}\|^2 < \frac{1}{2}\|\mathbf{g}\|^2.
 \end{aligned} \tag{16}$$

Therefore, combining (12)–(16) the proof is completed. 

We use the standard argument for finite elements and introduce the linear nodal interpolate  $I_h\mathbf{u} \in \mathbf{U}_h$  of the exact solution  $\mathbf{u}$  and we set  $\eta = \mathbf{u} - I_h\mathbf{u}$  and  $\xi = \mathbf{u}_h - I_h\mathbf{u}$ . Thus,

$$\zeta := \mathbf{u} - \mathbf{u}_h = (\mathbf{u} - I_h\mathbf{u}) - (I_h\mathbf{u} - \mathbf{u}_h) = \eta - \xi.$$

Recalling the Galerkin orthogonality relation

$$B(\zeta, \mathbf{u}) = 0. \tag{17}$$

Now we prove the basic global error estimate by using Proposition 1.

**Proposition 2.** *If  $\mathbf{u}_h \in \mathbf{U}_h$  satisfies (8) and  $\mathbf{u} \in \mathbf{H}^{k+1}(\Omega)$  with  $k \geq 1$  is exact solution (4) and also*

$$\|\mathbf{u}\|_\infty + \|\mathbf{F}(\mathbf{u})\|_\infty + \|\nabla\eta\|_\infty \leq C,$$

then there is a constant  $C$  such that

$$\|\mathbf{u} - \mathbf{u}_h\| \leq Ch^{k+1/2} \|\mathbf{u}\|_{k+1,\Omega}. \quad (18)$$

**Proof:** Using the definition of  $\eta$  we write

$$\begin{aligned} & \mathbf{B}(\mathbf{F}(\mathbf{u}); \mathbf{u}, \xi) - \mathbf{B}(\mathbf{F}(\mathbf{u}_h); \mathbf{I}_h\mathbf{u}, \xi) \\ &= \mathbf{B}(\mathbf{F}(\mathbf{u}_h); \eta, \xi) + \mathbf{B}(\mathbf{F}(\mathbf{u}); \mathbf{u}, \xi) - \mathbf{B}(\mathbf{F}(\mathbf{u}_h); \mathbf{u}, \xi) := T_1 + T_2 - T_3. \end{aligned}$$

Now we estimate the terms  $T_1$  and  $T_2 - T_3$  separately. For the term  $T_1$  we use the inverse inequality, therefore

$$\begin{aligned} T_1 &= \mathbf{B}(\mathbf{F}(\mathbf{u}_h); \eta, \xi) = (\eta_t + \mathbf{F}(\mathbf{u}_h)\eta, \xi + \delta(\xi_t + \mathbf{F}(\mathbf{u}_h)\xi))_\Omega + \frac{1}{2}(\mathbf{A}\nabla\eta, \nabla\xi)_\Omega \\ &\quad - \frac{1}{2}\delta(\mathbf{A}\Delta\eta, \xi_t + \mathbf{F}(\mathbf{u}_h)\xi)_\Omega + \sum_{n=1}^{N-1} \langle [\eta], \xi_+ \rangle_n + \langle \eta_+, \xi_+ \rangle_0. \end{aligned}$$

By using property of  $\mathbf{F}$ , integrating by parts, and since  $\Omega$  is bounded with zero boundary condition we get

$$\begin{aligned} T_1 &= -(\eta, \xi_t + \mathbf{F}(\mathbf{u}_h)\xi)_\Omega + \delta(\eta_t + \mathbf{F}(\mathbf{u}_h)\eta, \xi_t + \mathbf{F}(\mathbf{u}_h)\xi)_\Omega + \frac{1}{2}(\mathbf{A}\nabla\eta, \nabla\xi)_\Omega \\ &\quad - \frac{1}{2}\delta(\mathbf{A}\Delta\eta, \xi_t + \mathbf{F}(\mathbf{u}_h)\xi)_\Omega + \langle \eta_-, \xi_- \rangle_N - \sum_{n=1}^{N-1} \langle \eta_-, [\xi] \rangle_n. \end{aligned}$$

We use inverse inequality and have

$$\begin{aligned} \frac{1}{2}|(\mathbf{A}\nabla\eta, \nabla\xi)_\Omega| &\leq \frac{1}{2}\|\mathbf{A}\nabla\eta\|_\Omega \|\nabla\xi\|_\Omega \\ &\leq C_1\|\nabla\eta\|_\Omega \|\nabla\xi\|_\Omega \leq Ch^{-1}\|\eta\|_\Omega^2 + \|\nabla\xi\|_\Omega^2, \quad (19) \end{aligned}$$

and

$$\begin{aligned} \frac{1}{2}\delta|(A\Delta\eta, \xi_t + F(\mathbf{u}_h)\xi)_\Omega| &\leq \frac{1}{2}\delta\|A\Delta\eta\|_\Omega\|\xi_t + F(\mathbf{u}_h)\xi\|_\Omega \\ &\leq \frac{1}{2}\delta\|\eta\|_\Omega\|\xi_t + F(\mathbf{u}_h)\xi\|_\Omega \leq Ch^{-1}\|\eta\|_\Omega^2 + \frac{\delta}{2}\|\xi_t + F(\mathbf{u}_h)\xi\|_\Omega^2. \end{aligned} \quad (20)$$

By using (19) and (20) and a similar argument as in the proof of Proposition 1,


$$|T_1| \leq \frac{1}{2}\|\xi\|^2 + C \left\{ h^{-1}\|\eta\|_\Omega^2 + h\|\eta_t + F(\mathbf{u}_h)\eta\|_\Omega^2 + |\eta_-|_N^2 + \sum_{n=1}^{N-1} |\eta_-|_n^2 \right\}. \quad (21)$$

To estimate the term  $T_2 - T_3$ , we follow a similar argument to Adams [1]:

$$\begin{aligned} |T_2 - T_3| &= |(\mathbf{u}_t + F(\mathbf{u})\mathbf{u}, \xi + \delta(\xi_t + F(\mathbf{u}_h)\xi))_\Omega \\ &\quad - (\mathbf{u}_t + F(\mathbf{u}_h)\mathbf{u}, \xi + \delta(\xi_t + F(\mathbf{u}_h)\xi))_\Omega| \\ &= |(F(\mathbf{u}) - F(\mathbf{u}_h))\mathbf{u}, \xi + \delta(\xi_t + F(\mathbf{u}_h)\xi))_\Omega| \\ &\leq \|F(\mathbf{u}) - F(\mathbf{u}_h)\|_\Omega\|\mathbf{u}\|_\infty\|\xi\|_\Omega + Ch\|F(\mathbf{u}) - F(\mathbf{u}_h)\|_\Omega^2\|\mathbf{u}\|_\infty^2 \\ &\quad + \frac{Ch}{8}\|\xi_t + F(\mathbf{u}_h)\xi\|_\Omega^2. \end{aligned} \quad (22)$$

By using the definition of  $F$ ,

$$\|F(\mathbf{u}) - F(\mathbf{u}_h)\|_\Omega \leq C\|\mathbf{u} - \mathbf{u}_h\|_\Omega \leq C(\|\xi\|_\Omega + \|\eta\|_\Omega). \quad (23)$$

Now we combine the estimates (21)–(23), therefore  $\|\xi_t + F(\mathbf{u}_h)\xi\|_\Omega^2$  and the proof is completed. 

## 4 Experimental results

This section presents two numerical examples of the proposed scheme (8). To motivate the work of the streamline diffusion method, we present a non-smooth solution. The accuracy of the new SD-method is tested by looking at

the error using  $L_2$  norm, which is an important feature of smooth solutions. In Tables 1 and 2 we observe that the accuracy of this scheme is better than other methods (that is, CN, FE, CG, DG and DPG) by comparing the numerical solution with the exact solution at each time level. We know that equations (1)–(4) admit two stationary solutions:

$$\begin{aligned} \psi_1(x_1, x_2, x_3, t) &= \sqrt{\frac{2\alpha}{1+e}} \operatorname{sech} \left\{ \sqrt{\alpha} \left( \sqrt{x_1^2 + x_2^2 + x_3^2} - 2vt \right) \right\} \\ &\quad \times \exp \left( i \left\{ v \sqrt{x_1^2 + x_2^2 + x_3^2} - [v^2 - \alpha]t \right\} \right), \\ \psi_2(x_1, x_2, x_3, t) &= \pm \sqrt{\frac{2\alpha}{1+e}} \operatorname{sech} \left\{ \sqrt{\alpha} \left( \sqrt{x_1^2 + x_2^2 + x_3^2} - 2vt \right) \right\} \\ &\quad \times \exp \left( i \left\{ v \sqrt{x_1^2 + x_2^2 + x_3^2} - [v^2 - \alpha]t \right\} \right), \end{aligned}$$

where  $x_L = -20$ ,  $x_R = 20$ ,  $h = 0.1$ ,  $v = 1.0$ ,  $\alpha = 1.0$ , and for having a non-smooth solution we assume the following two cases:

**Case 1** for  $T = 0.5$ ,

$$e(t) = \begin{cases} 1.0 & t > 0.3, \\ 0.0 & t \leq 0.3; \end{cases} \quad (24)$$

**Case 2** for  $T = 1.0$ ,

$$e(t) = \begin{cases} e^{t^2-1} & t > 0.5, \\ \sin t & t \leq 0.5. \end{cases} \quad (25)$$

Also, the accuracy is measured by  $L_2$  error norm defined by

$$\|\zeta(h)\| = \|\mathbf{u} - \mathbf{u}_h\| = \sqrt{h \sum_j^M \left| \mathbf{u} \left( x_1^j, x_2^j, x_3^j, t \right) - \mathbf{u}_{hj} \right|^2}.$$

The order of error is calculated using

$$\text{Order of error} \approx \frac{\ln(\zeta(h))}{\ln h}.$$

We carry out (9) on an AMD Opteron computer with 15 GB RAM memory with 2.2 GHz CPU for these experiments. For each slab  $S_n$ , we consider a mesh. For  $h > 0$  let  $T_h^n$  be a triangulation of the slab  $S_n$  into triangle  $K$ , satisfying as usual the minimum angle condition [30]. The triangulation of  $S_n$  may be chosen independently of that of  $S_{n-1}$ , but for the sake of simplicity it must satisfy quasi-uniformity conditions for finite element meshes [7, 8, 9, 10]. To give numerical results obtained using the new SD-method, we use finite element approximation on a space-time slab with trial functions which are piecewise polynomials in space and linear in time. That is, for  $x = (x_1, x_2, x_3, t) \in S_n$ ,

$$\begin{aligned} \text{Imag}(\psi_{1,h})^n(x, t) &= \sum_{i=1}^M \varphi_i(x)(\theta_1(t)\tilde{u}_{1,i}^n + \theta_2(t)u_{1,i}^{n+1}), \\ \text{Imag}(\psi_{2,h})^n(x, t) &= \sum_{i=1}^M \varphi_i(x)(\theta_1(t)\tilde{u}_{2,i}^n + \theta_2(t)u_{2,i}^{n+1}), \\ \text{Real}(\psi_{1,h})^n(x, t) &= \sum_{i=1}^M \varphi_i(x)(\theta_1(t)\tilde{u}_{3,i}^n + \theta_2(t)u_{3,i}^{n+1}), \\ \text{Real}(\psi_{2,h})^n(x, t) &= \sum_{i=1}^M \varphi_i(x)(\theta_1(t)\tilde{u}_{4,i}^n + \theta_2(t)u_{4,i}^{n+1}), \end{aligned} \quad (26)$$

such that  $\varphi_i(x^j) = \delta_{ij}$ , ( $j = 1, \dots, M$ ) is the spatial shape functions at node  $i$ ,  $\theta_1(t)$  and  $\theta_2(t)$  are the time interpolation functions defined for Bézier curves. Also, the nodal value of  $\mathbf{u}$  for node  $i$  at  $(t_n)_+$  and  $(t_{n+1})_-$  are denoted by  $\tilde{\mathbf{u}}_i^n$  and  $\mathbf{u}_i^{n+1}$ . The test functions  $\mathbf{g}_i^n$  for each time slab are defined as  $\varphi_j(x)\theta_1(t)$  and  $\varphi_j(x)\theta_2(t)$  for  $j = 1, \dots, M$ .

The error of theSD-method and other methods with exact solutions for the image part and real part are compressed into Table 1 by  $L_2$  norm, for Case 1. Also, we repeat the results for Case 2 in Table 2. Hence, the evolution of error by different methods, at the given time and  $\delta$  are given in Tables 1–2. Moreover, Figure 2 plots the  $L_2$  errors for the terminating time  $T = 0.5$ ,  $k = 0.001$  and  $\delta = 0.01$  as a function of CPU time for the new SD-method.

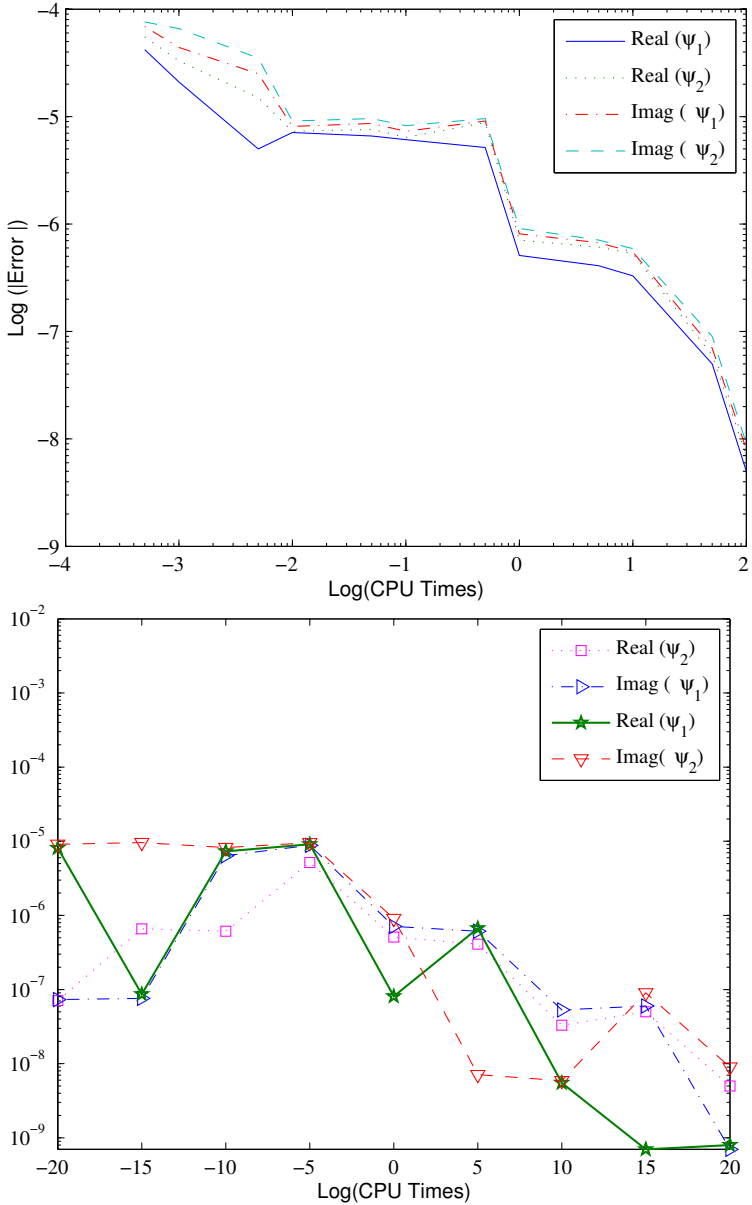


Figure 2: The  $L_2$  errors for percentage of terminating time,  $\delta = 0.01$ , as a function of CPU time for the new SD-method for Case 1 (top) and Case 2 (bottom).



Table 1:  $L_2$  error for  $h = 0.1$  and time step  $0.01$  by different methods for  $t = 0.3$  in Case 1. The SD method is for  $\delta = 0.00125$ .

| $x$               | CN     | CG     | FE     | DG      | DPG     | SD      |
|-------------------|--------|--------|--------|---------|---------|---------|
| $(-20, -20, -20)$ | 1.8E-5 | 6.2E-5 | 1.3E-9 | 1.5E-9  | 1.1E-10 | 3.2E-11 |
| $(-20, -20, 20)$  | 2.1E-6 | 6.1E-6 | 3.5E-8 | 7.3E-10 | 2.7E-10 | 2.4E-10 |
| $(-20, 20, -20)$  | 7.2E-6 | 7.7E-6 | 3.8E-8 | 6.5E-10 | 7.4E-10 | 9.5E-10 |
| $(20, -20, -20)$  | 6.4E-6 | 8.8E-6 | 4.0E-8 | 0.8E-10 | 6.5E-10 | 8.3E-11 |
| $(20, 20, -20)$   | 7.3E-6 | 5.9E-6 | 1.8E-8 | 8.5E-10 | 2.9E-10 | 7.6E-10 |
| $(20, -20, 20)$   | 3.2E-6 | 6.4E-6 | 9.4E-8 | 7.3E-10 | 8.7E-11 | 7.6E-11 |
| $(-20, 20, 20)$   | 5.1E-5 | 3.3E-6 | 6.5E-9 | 5.9E-10 | 3.3E-10 | 2.6E-10 |
| $(20, 20, 20)$    | 2.3E-5 | 2.6E-5 | 2.0E-8 | 6.5E-9  | 8.4E-10 | 4.1E-11 |
| order             | 2.1    | 2.9    | 3.4    | 3.9     | 3.9     | 4.4     |

*Remark 3.* In the FE method, we choose linear spline functions as basis functions. For the all methods in the tables, the fourth order Runge–Kutta method is used to solve the system of ODE at each time level. In the CG we use trial functions which are piecewise linear and continuous whereas the test functions are piecewise constant and discontinuous. In particular, all the analysis is made taking the parameter  $\delta = 0$ , and therefore the method analyzed is the discontinuous Galerkin (DG) method [32], not the streamline diffusion method. In the DG and SD-methods we consider that both the trial and test functions are piecewise linear and discontinuous. The compound trapezoidal integral formula computes the integration in coefficient matrices in the above methods. Also, we use the algorithm of DPG form [36]. A useful book for constructive algorithms was written by Yang [34].

Based on the numerical results of others [29, 30, 37], we observe that the new SD-scheme is better than the finite difference methods and standard finite element by comparing the numerical solution with the exact solution. The agreement of the error estimates between theoretical analysis and numerical

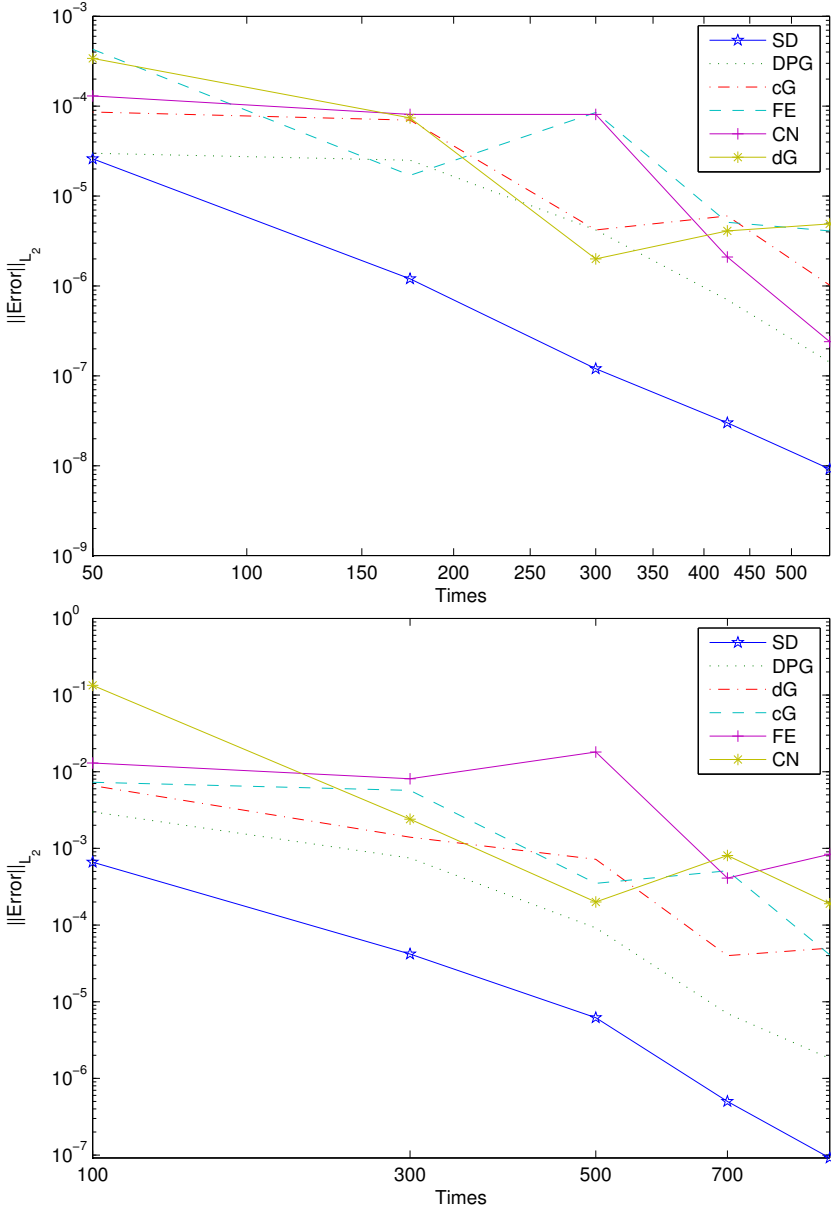


Figure 3: Comparison of CPU time for the different schemes when the  $L_2$  errors for percentage of terminating time for Case 1 (top) and Case 2 (bottom).

Table 2:  $L_2$  error for  $h = 0.1$  and time step  $0.01$  by different methods for  $t = 0.5$  in Case 2. The SD method is for  $\delta = 0.00125$ .

| $\mathbf{x}$      | CN     | CG     | FE     | DG      | DPG     | SD      |
|-------------------|--------|--------|--------|---------|---------|---------|
| $(-20, -20, -20)$ | 6.2E-6 | 4.7E-6 | 2.0E-8 | 3.4E-9  | 1.2E-9  | 7.6E-10 |
| $(-20, -20, 20)$  | 7.5E-5 | 4.2E-6 | 5.1E-8 | 2.6E-10 | 7.6E-10 | 5.0E-10 |
| $(-20, 20, -20)$  | 3.1E-7 | 7.4E-6 | 5.4E-9 | 1.8E-10 | 1.0E-9  | 5.6E-10 |
| $(20, -20, -20)$  | 7.0E-5 | 1.0E-5 | 3.2E-8 | 2.3E-9  | 8.7E-11 | 4.1E-11 |
| $(20, 20, -20)$   | 7.0E-6 | 5.0E-6 | 1.8E-8 | 8.7E-10 | 8.9E-10 | 1.6E-10 |
| $(20, -20, 20)$   | 1.0E-6 | 9.7E-6 | 1.9E-8 | 9.8E-10 | 9.6E-10 | 4.5E-10 |
| $(-20, 20, 20)$   | 8.9E-6 | 5.4E-6 | 9.8E-8 | 1.0E-10 | 7.8E-10 | 1.0E-10 |
| $(20, 20, 20)$    | 1.2E-7 | 2.8E-6 | 8.9E-8 | 1.0E-9  | 5.6E-10 | 3.2E-10 |
| order             | 2.1    | 2.5    | 3.3    | 3.9     | 3.9     | 4.8     |

results shows that our method is efficient. We know that CPU time (or process time) is measured in clock ticks or seconds. Therefore, in Figure 2, we report CPU times for this equation by the new SD-method. Here, we observe that CPU times and  $L_2$  errors have similar behaviours. Also we give Figure 3, since there needs to be a comparison, across the different numerical schemes, of CPU (computational effort) for the given fixed accuracy and it is useful to measure CPU time as a percentage of the CPU's capacity, which is called the CPU usage. Hence, we observe that the behaviour of CPU time and CPU usage in the new SD algorithm are better than others. For Figures 4-7, we consider that  $\mathbf{X} = \frac{1}{3} \sum_{j=1}^3 \mathbf{x}_j$  and  $\delta = 0.01$  for Case 1 and Case 2 respectively. In particular, the surfaces of  $\mathbf{e}_i$  in Figures 4-7 only produce very little difference. The reason maybe due to that the error order of the new SD-method is close to four, whereas the error order is two on CN method and the error order is three on the DG, FE, CG, DPG methods. The agreement of the error estimates between theoretical analysis and numerical results shows that our method is efficient.

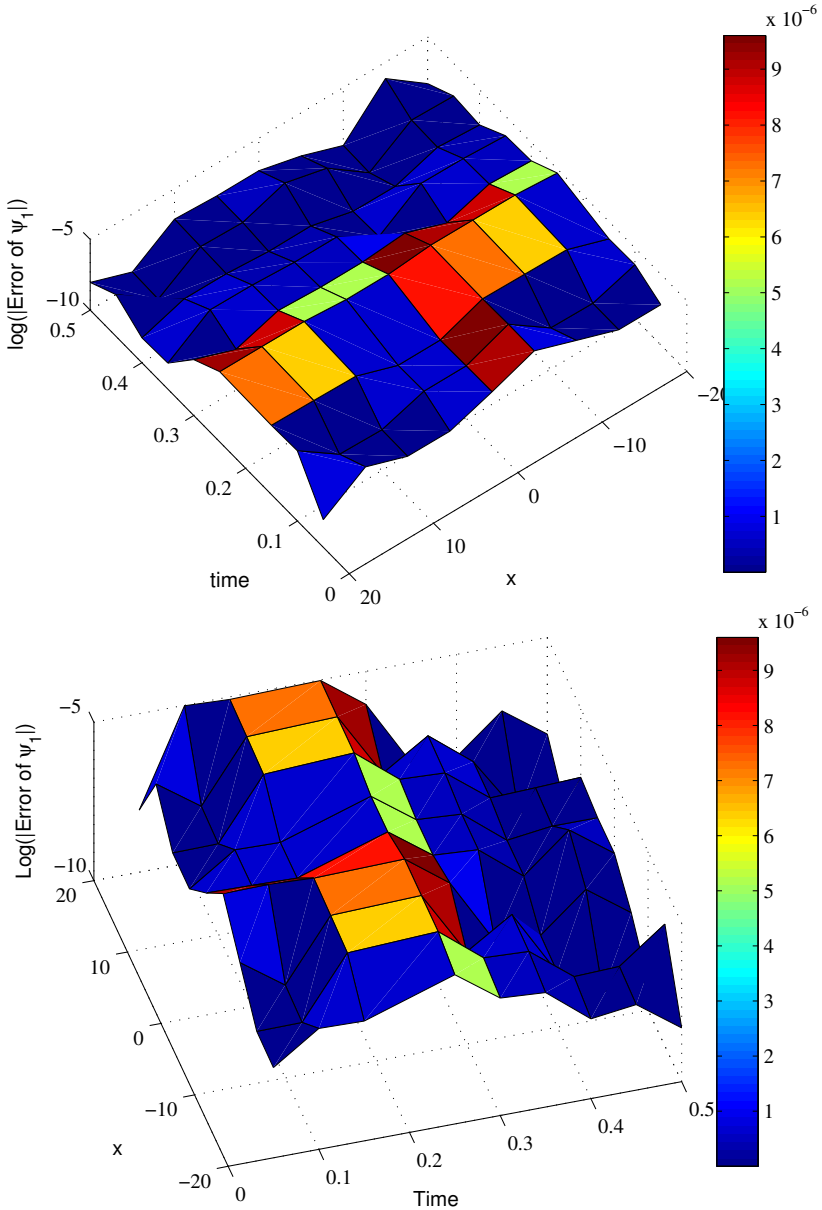


Figure 4: The absolute error of the new SD-method for the imaginary part of  $\psi_1$  (top), the real part of  $\psi_1$  (bottom) when  $X = \frac{1}{3} \sum_{j=1}^3 x_j$  and  $\delta = 0.01$  for Case 1.

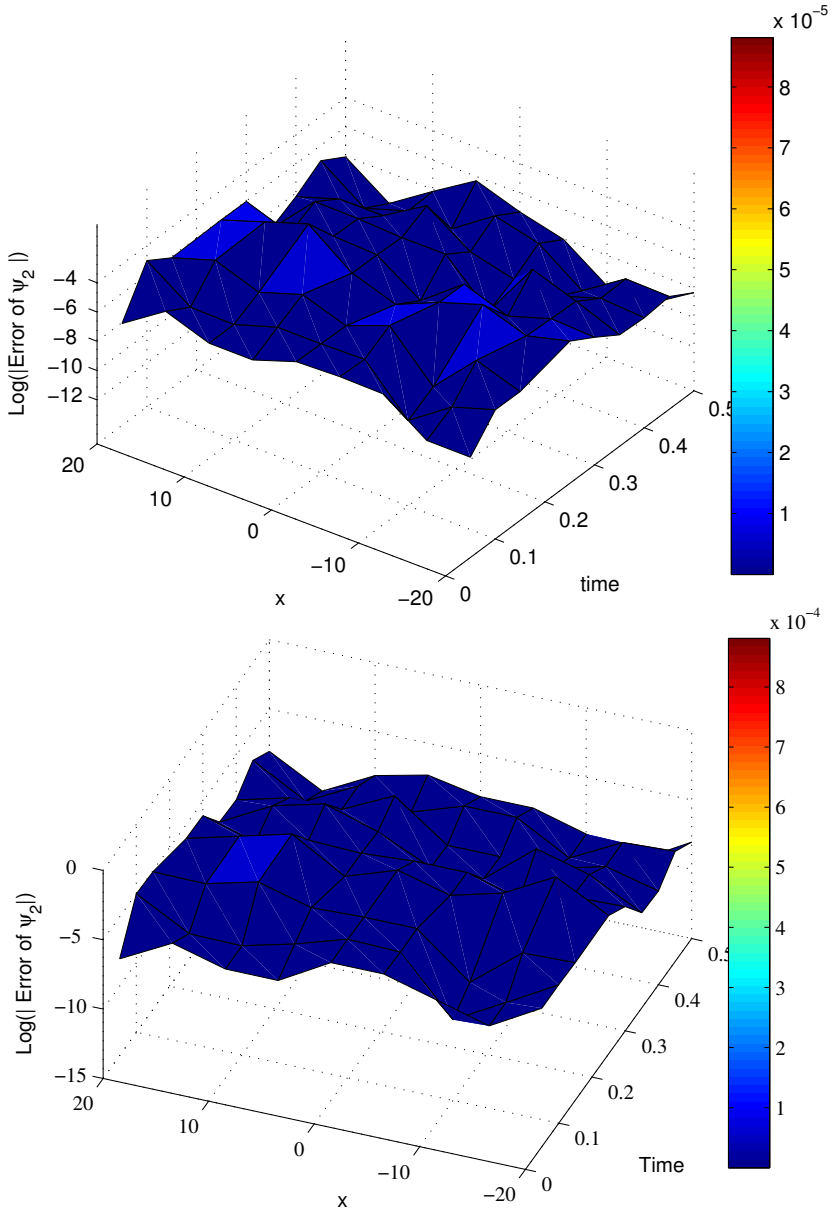


Figure 5: The absolute error of the new SD-method for the imaginary part of  $\psi_2$  (top) and the real part of  $\psi_2$  (bottom) when  $X = \frac{1}{3} \sum_{j=1}^3 x_j$  and  $\delta = 0.01$  for Case 1.

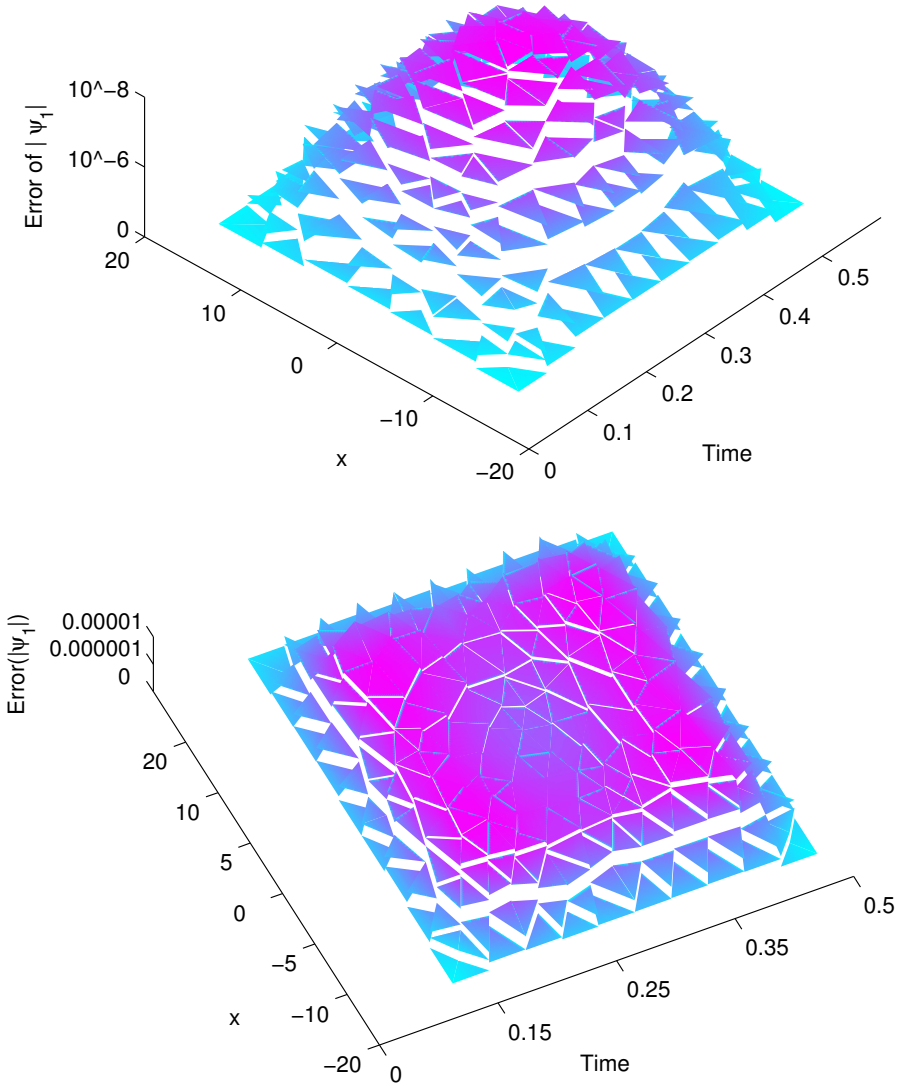


Figure 6: The absolute error of SD- method for the imaginary part of  $\psi_1$  (top), the real part of  $\psi_1$  (bottom) when  $X = \frac{1}{3} \sum_{j=1}^3 x_j$  and  $\delta = 0.01$  for Case 2.

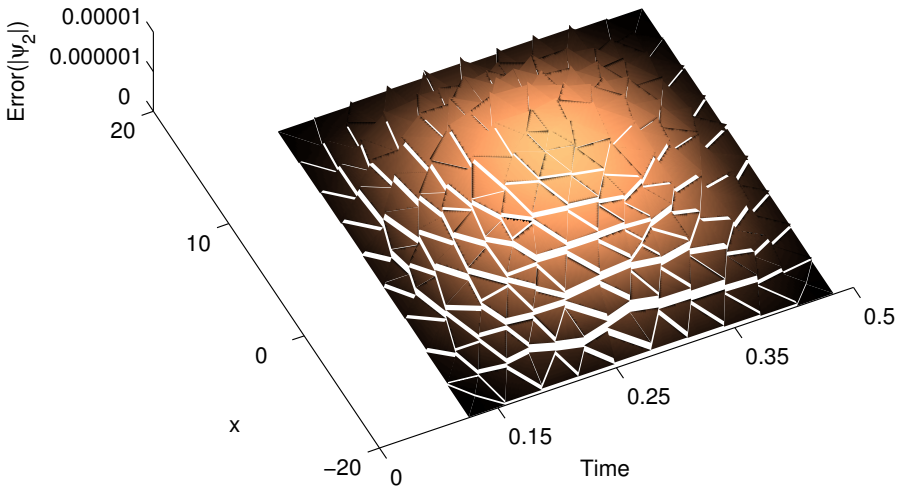
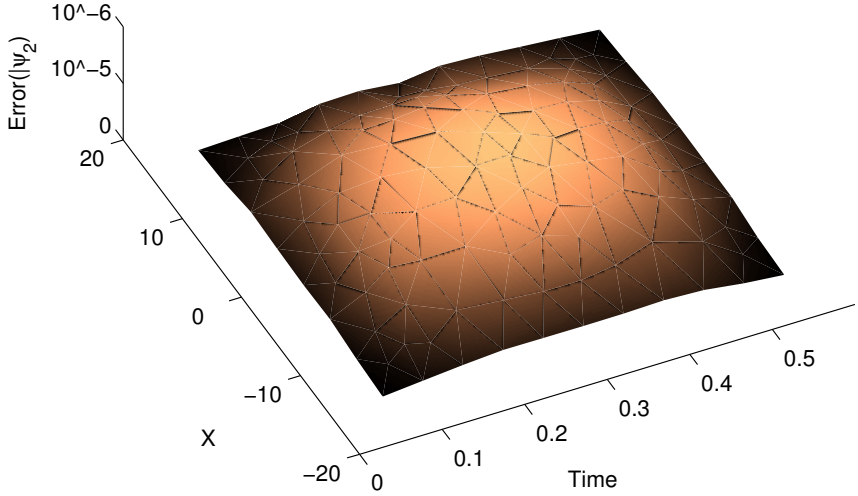


Figure 7: The absolute error of SD- method for the imaginary part of  $\psi_2$  (top) and the real part of  $\psi_2$  (bottom) when  $X = \frac{1}{3} \sum_{j=1}^3 x_j$  and  $\delta = 0.01$  for Case 2.

## 5 Conclusion

The streamline diffusion is developed by solving coupled nonlinear Schrödinger equations with non-smooth coefficient. This cannot be as a simple application of streamline diffusion because we can obtain the optimal convergence rate for the new SD-method that is  $\mathcal{O}(h^{k+1/2})$ . Recently, powerful stabilization techniques were introduced [25, 26, 28, 36], but for this equation, they are weak. The numerical results confirm that the new SD-method is more efficient than other methods for this equation. The theory is illustrated by a numerical example and the superior accuracy of this scheme is shown by comparing the numerical solutions with the exact solutions. A posteriori error estimate remains a challenge that deserves special attention and will be considered elsewhere.

**Acknowledgements** I thank anonymous referee whose constructive comments improved the quality of this paper and finally it is a pleasure to acknowledge the skilful editorial assistance from the Series Editor of this journal, Anthony John Roberts.

## References

- [1] R. A. Adams, *Sobolev Spaces*, Academic Press, New York (1975). E58, E63
- [2] J. Albery, C. Carstensen, Discontinuous Galerkin Time Discretization in Elastoplasticity: Motivation, Numerical Algorithms, and Applications, *Comput. Methods Appl. Mech. Engrg.*, 191(2002), 43, 4949–4968. E53
- [3] M. Asadzadeh, D. Rostamy, F. Zabihi, Discontinuous Galerkin and multiscale variational schemes for a coupled damped nonlinear system of



- Schrödinger equations, *Numerical Methods for Partial Differential Equations*, APR 2013 doi:[10.1002/num.21782](https://doi.org/10.1002/num.21782) E53
- [4] M. Asadzadeh, D. Rostamy and F. Zabihi, A posteriori error estimates for the solutions of a coupled wave system, *Journal of Mathematical Sciences*, Vol. 175, No. 2 (2011) pp. 228–248. E53
- [5] S. C. Brenner and L. R. Scott, *The Mathematical Theory of Finite Element Method*, Springer–Verlag, New York, (1994). E53
- [6] E. Burman, Adaptive Finite Element Methods for Compressible Two–Phase Flow, *Math. Mod. Meth. App. Sci.*, 10 (2000), pp. 963–989. E53
- [7] C. Carstensen, M. Jensen, Th. Gudi, A unifying theory of a posteriori error control for discontinuous Galerkin FEM, *Numer. Math.*, 112, 3 (2009), pp. 363–379. E53, E65
- [8] C. Carstensen, G. Dolzmann, An a priori error estimate for finite element discretizations in nonlinear elasticity for polyconvex materials under small loads, *Numer. Math.*, 97(2004), 67–80. E53, E65
- [9] P. G. Ciarlet, *The Finite Element Method for Elliptic Problems*, Amsterdam, North Holland, (1987). E53, E57, E65
- [10] R. Codina, Finite element approximation of the hyperbolic wave equation in mixed form, *Comput. Methods Appl. Mech. Engrg.*, 197 (2008), pp. 1305–1322 E52, E53, E65
- [11] F. Dubois and P. G. Le Floch, Boundary conditions for nonlinear hyperbolic systems of conservation laws, *J. Differential Equations*, 71 (1988), pp. 93–122. E52
- [12] K. Eriksson, C. Johnson, Adaptive Streamline Diffusion Finite Element Methods for Stationary Convection-Diffusion Problems, *Math. Comp.*, 60 (1993), pp. 167–188. E53

- [13] K. Eriksson and C. Johnson, Adaptive finite element methods for parabolic problems I: A linear model problem, *SIAM J. Numer. Anal.*, 28 (1991), pp. 43–77. MR 91m:65274. [E53](#)
- [14] K. Eriksson and C. Johnson, Adaptive finite element methods for parabolic problems II: Optimal error estimates in  $L_\infty L_2$  and  $L_\infty L_\infty$ , *SIAM J. Numer. Anal.*, 32 (1995), pp. 706–740. MR 96c:65162. [E53](#)
- [15] K. Eriksson and C. Johnson, Adaptive finite element methods for parabolic problems IV: A nonlinear problem, *SIAM J. Numer. Anal.*, 32 (1995), pp. 1729–1749. MR 96i:65081. [E53](#)
- [16] K. Eriksson, C. Johnson and V. Thomee, Time discretization of parabolic problems by the Discontinuous Galerkin method, *RAIRO, Anal. Numer.*, 19 (1985), pp. 611–643. MR 87e:65073. [E53](#)
- [17] C. Fuhrer and R. Rannacher, An Adaptive Streamline Diffusion Finite Element Method for Hyperbolic Conservation Laws, *East-West J. Numer. Math.*, 5 (1997), pp. 145–162. [E53](#)
- [18] E. H. Gergoulus, O. Lakkis and C. Makridakis, A posteriori  $L^\infty(L^2)$ -error bounds in finite element approximation of the wave equation, [arXiv:1003.3641v1](#) (2010). [E53](#)
- [19] E. Godlewski and P. Raviart, The numerical interface coupling of nonlinear hyperbolic systems of conservation laws: I. The scalar case, *Numer. Math.*, 97 (2004), pp. 81–130. [E52](#), [E53](#)
- [20] M. S. Ismail, Numerical solution of coupled nonlinear Schrödinger equation by Galerkin method, *Mathematics and Computers in Simulation*, 78 (2008) pp. 532–547. [E53](#), [E55](#)
- [21] M. S. Ismail and T. R. Taha, A linearly implicit conservative scheme for the coupled nonlinear Schrödinger equation, *Math. Comp. Simul.*, 74 (2007) pp. 302–311. [E53](#), [E55](#)

- [22] M. S. Ismail and S. Z. Alamri, Highly accurate finite difference method for coupled nonlinear Schrödinger equation, *Int. J. Comput. Math.*, 81 (3) (2004) pp. 333–351. [E53](#), [E55](#)
- [23] M. S. Ismail, T. Taha, Numerical simulation of coupled nonlinear Schrödinger equation, *Math. Comput. Simul.*, 56 (2001) pp. 547–562. [E53](#), [E55](#)
- [24] M. S. Ismail, T. Taha, A finite element solution for the coupled Schrödinger equation, in: *Proceedings of the 16th IMACS World Congress on Scientific Computation*, Lausanne, (2000). [E52](#), [E53](#), [E55](#)
- [25] M. Izadi, *Streamline diffusion Finite Element Method for coupling equations of nonlinear hyperbolic scalar conservation laws*, MSc Thesis, (2005). [E53](#), [E74](#)
- [26] M. Izadi, A posteriori error estimates for the coupling equations of scalar conservation laws, *BIT Numer. Math.*, 49(2009), pp. 697–720. [E53](#), [E74](#)
- [27] C. Johnson and A. Szepessy, Adaptive Finite Element Methods for Conservation Laws Based on a posteriori Error Estimates, *Comm. Pure. Appl. Math.*, 48 (1995), pp. 199–234. [E53](#)
- [28] C. Johnson, *Numerical solutions of partial differential equations by the Finite Element Method*, CUP, (1987). [E53](#), [E58](#), [E74](#)
- [29] C. Johnson and J. Pitkaranta, An analysis of the Discontinuous Galerkin method for a scalar hyperbolic equation, *Math. comput.*, 46 (1986), pp. 1–26. [E53](#), [E67](#)
- [30] C. Johnson, Discontinuous Galerkin finite element methods for second order hyperbolic problems, *Comput. Methods Appl. Mech. Engg.*, 107 (1993), pp. 117–129. [E53](#), [E65](#), [E67](#)
- [31] M. Wadati, T. Izuka, M. Hisakado, A coupled nonlinear Schrödinger equation and optical solitons, *J. Phys. Soc. Jpn.*, 61 (7) (1992), pp. 2241–2245. [E53](#), [E55](#)

- [32] Y. Xu, C. Shu, Local discontinuous Galerkin method for nonlinear Schrödinger equations, *J. Comput. Phys.*, 205 (2005), pp. 72–97. [E53](#), [E67](#)
- [33] J. Yang, A tail–matching method for the linear stability of multi-vector-soliton bound states, *Contemporary Mathematics*, Volume 379 (2005) pp.63–82. [E52](#), [E53](#), [E55](#)
- [34] J. Yang, Nonlinear waves in integrable and nonintegrable system, *SIAM*, 2010. [E52](#), [E53](#), [E67](#)
- [35] D. Wang, Da Jun Zhang and Z. Yang, Integrable properties of the general couple nonlinear Schrödinger equations, *Journal of Mathematical Physics*, 51 (2010) pp. 121–134. [E53](#)
- [36] M. J. Borden, M. A. Scott, J. A. Evans, T. J. R. Hughes ,Isometric finite element data structures based on Bézier extraction of NURBS, *Int. J. numer. Math. Engng.*, 87 (2011) 15–47. [E53](#), [E56](#), [E67](#), [E74](#)
- [37] J. Zitelli, I. Muga, L. Demkowicz , J. Gopalakrishnan, D. Pardo, V. M. Calo, A class of discontinuous Petrov–Galerkin methods. Part IV: The optimal test norm and time-harmonic wave propagation in 1D, *Journal of Computational Physics*, 230 (2011) 2406–2432. [E53](#), [E55](#), [E67](#)

## Author address

1. **Davood Rostamy**, Department of Mathematics, Imam Khomeini International University, Qazvin, Iran. Tel. +9821-44870779; Fax +9821-44802601  
<mailto:rostamy@khayam.ut.ac.ir>